ACS Catalysis

Research Article

pubs.acs.org/acscatalysis

Platinum Nanoclusters Stabilized on γ-Alumina by Chlorine Used As a Capping Surface Ligand: A Density Functional Theory Study

C. Mager-Maury,[1,2] C. Chizallet,[1] P. Sautet,[2,*] and P. Raybaud[1,*]

[1]IFP Energies Nouvelles, Rond-point de l'échangeur de Solaize, BP 3-69360 Solaize, France

[2]Université de Lyon, CNRS, Laboratoire de Chimie, Ecole Normale Supérieure de Lyon, 46 allée d'Italie, 69364 Lyon cedex 07, France

Supporting Information

ABSTRACT: Controlling the size of metallic nanoclusters supported on an oxide support such as γ-alumina represents a challenging but important task in the case of noble metals such as platinum. By using density functional theory (DFT), we investigate the thermodynamic, structural and electronic properties of small nanometer-sized Pt_n clusters ($n \leq 13$) interacting with four relevant γ-alumina surfaces exhibiting various hydroxylation and chlorination states. The presence of chlorine on the (110) surface of γ-alumina implies a thermodynamic stabilization of small platinum clusters. This stabilization originates from the simultaneous migrations of chlorine atoms and protons from the support toward the Pt clusters. The migration of H and Cl from the support induces a stronger interaction of the Pt_n cluster with the available Al_{III} site, associated with strong H−Pt_n−Cl interaction. In particular, this trend leads to a local energy minimum, as a function of cluster size, for the Pt_3 cluster. This atomic-scale stabilization of subnanometer clusters is thus proposed to be at the origin of the formation of highly dispersed platinum particles and to prevent their sintering into supranano ones. A detailed energetic and electronic analysis is provided to rationalize this effect of chlorine. A rational interpretation of experimental data is finally given.

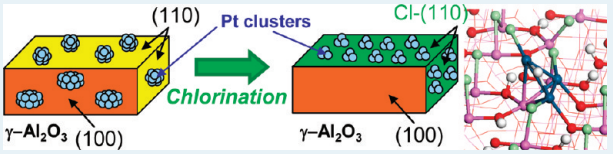

KEYWORDS: *particles, platinum, chlorine, alumina, migration, density functional theory*

INTRODUCTION

The control of the size of metallic particles is a fundamental question with a large array of applications in catalysis, nanoscience, information storage, and magnetism.[1−6] Small, bare metallic particles naturally tend to sinter into larger ones to increase the coordination number of the metal atoms. Hence, their stabilization at a given size is highly challenging but fundamental for applications. In particular, subnanometer-sized metal particles present very specific electronic and chemical properties.[7,8] They also present the advantage of an optimal dispersion, nearly all the atoms being present at the surface, which is important for economical reasons in the case of rare transition metals such as Pt or Rh. Hence, the understanding of the mechanisms that allow the stabilization of small particles is a key aspect for many application fields.[1,9]

There are several ways to reach this goal. One is to use ligand molecules, which allows the control of the growth of the particles, such as in colloid science.[10] Another common approach is to use a high-surface-area solid support, such as a metal oxide, to kinetically favor small particles. This approach is used in heterogeneous catalysis, in which the optimal stabilization of small particles by the support is of major importance to slow down the unavoidable sintering in larger particles and the loss of catalytic activity. Understanding how the support and its chemical nature control the particle stability as a function of size is, hence, of key importance for the rational design of well controlled, monodispersed, supported catalysts.

In particular, platinum supported on γ-alumina (γ-Al_2O_3) is a prominent catalyst involved in many different fields, such as the treatment of automobile exhaust,[11] reforming in the petroleum industry,[12] fuel cell technologies,[13] and biomass conversion.[14] The γ polymorph of alumina is the most widely used in industry because of its advantageous porosity, surface area, and chemical properties.[15] Catalytic reforming is one of the applications of interest in which subnanometer-sized particles are of great importance.[12] In this case, Pt is usually highly dispersed (content slightly lower than 1 wt %). Regarding the chemical nature of the alumina support, at least two synthesis and pretreatment parameters play a major role. The temperature is a key factor to monitor the remaining hydroxylation content of the alumina surface, and additives such as chlorine are strongly suspected to influence the particle size distribution. Chlorine can be either directly added on the alumina support or introduced by impregnation of H_2PtCl_6 acidic precursors in the Pt particle synthesis step. A typical Cl content of the alumina support is around 1 wt %. Chlorination treatments increase the acidity of the support but are also known to help maintain a high dispersion by decreasing the sintering effect observed during reaction.[12,16,17] However, the role of Cl in the stability of the subnanometer particles as well as the interactions between Cl species and the metallic aggre-

Received: March 17, 2012
Revised: May 10, 2012
Published: May 16, 2012

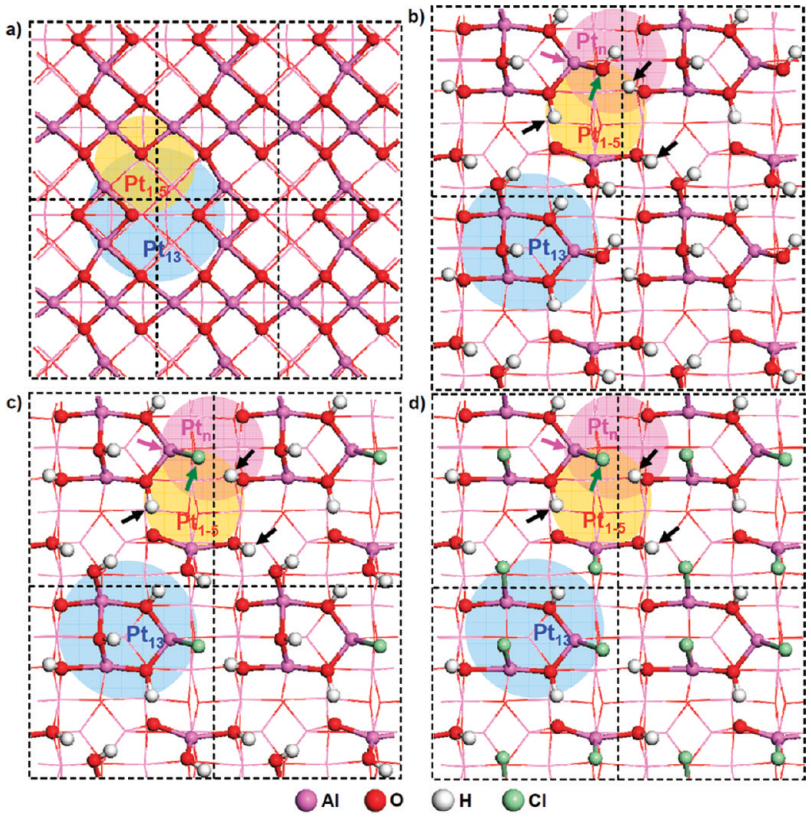

Figure 1. Top views of the γ-Al_2O_3 supercell models of (a) dehydrated (100) surface, (b) hydrated (110) surface, (c) slightly chlorinated (110) surface (1.5 Cl.nm^{-2}), and (d) highly chlorinated surface (5.9 Cl nm^{-2}). Optimal adsorption sites of Pt_n clusters: Pt_{1-5} without migration in orange disks, Pt_{13} without migration in blue disks, Pt_n with migration in pink disks. Relevant surface species involved in migration are marked with arrows (black, H atoms from surface hydroxyl groups; green, hydroxyl or chlorine group). Pink arrows mark the Al_{III} atom on the (110) surfaces. Dashed black lines delimit the irreducible unit cells while calculations are performed on (3 × 2) and (2 × 2) supercells, respectively, for the (100) and the (110) surfaces.

gates[16,18−20] remain mostly unknown. Hence, a better atomic scale characterization of these systems is required.

Regarding the metallic phase, microscopic techniques[19,21−23] provide an accurate characterization of two-dimensional projections of supported small clusters. For the investigation of the tridimensional atomic arrangement of small clusters, X-ray adsorption spectroscopy (XAS)[16,17,23−25] is a technique of choice and provides accurate data on Pt coordination numbers and distances to nearest neighbors. For example, in the case of 1 wt % Pt dispersed on γ-Al_2O_3, the coordination number of platinum (i.e., the average number of Pt neighbors) is 7.4, with a Cl loading of 1.1 wt %, whereas it decreases to 4 with 2.2 Cl wt % loading catalyst.[17] Even if particles as small as 0.6−1 nm, tentatively assigned to Pt_5 particles, were characterized by such techniques on γ-Al_2O_3,[17] XAS does not provide an unambiguous resolution of the particle 3D morphologies or a molecular-scale description of the chemical environment of the metallic clusters (interaction with the support and with adsorbed species). In particular, the precise location of chlorine remains a matter of debate: whereas some authors, on the basis of EXAFS measurements, argue that reduced Pt particles are not directly bound to chlorine,[16,19] some chlorinated Pt species were observed on reduced catalysts by TOF−SIMS (time-of-flight secondary ion mass spectrometry).[20]

The stabilization of small metal particles on a support is governed by the interaction with the oxide surface, hence partly compensating the bond insaturation at the edge of the cluster. Hence, the metal−support interactions were investigated at the molecular scale from first-principles calculations by several groups dealing with the adsorption of transition metals (TM) clusters such as Pt and Pd on α-Al_2O_3 and γ-Al_2O_3 supports.[26−36] Recently, we provided an atomic picture for Pt_{13} and Pd_{13} clusters supported on the dehydrated (100) and on the hydroxylated (110) surfaces of γ-Al_2O_3.[26] The importance of the hydroxylation level of the surface was pointed out. For TM clusters adsorbed on dehydrated surfaces, the metal−support interaction is ensured by formation of TM−O and TM−Al bonds, whereas on hydrated surfaces, TM atoms bond with O atoms from surface hydroxyl groups.

The challenging question we address in the present contribution is whether surface additives, such as chlorine, may improve the stability of small metallic particles and, if yes, by which mechanism. To our knowledge, the experimentally observed impact of surface chlorine doping on the dispersed metal has never been unambiguously demonstrated at a molecular scale. The aim of the present paper is thus to highlight and elucidate the role of chlorine for the size-dependent stability of Pt particles on alumina. For that purpose, we used density functional theory (DFT). From our previous study on hydroxylated and chlorinated surfaces, four relevant γ-alumina surfaces were selected for the adsorption of Pt_n clusters ($1 \leq n \leq 5$ and $n = 13$): the dehydrated (100) surface, the partially hydrated (110) γ-Al_2O_3 surface,[37,38] and two chlorinated (110) surfaces with different Cl concentrations.[39] A careful energetic and electronic analysis is then furnished, which helps for a rational interpretation. The results are

dx.doi.org/10.1021/cs300178y | ACS Catal. 2012, 2, 1346−1357

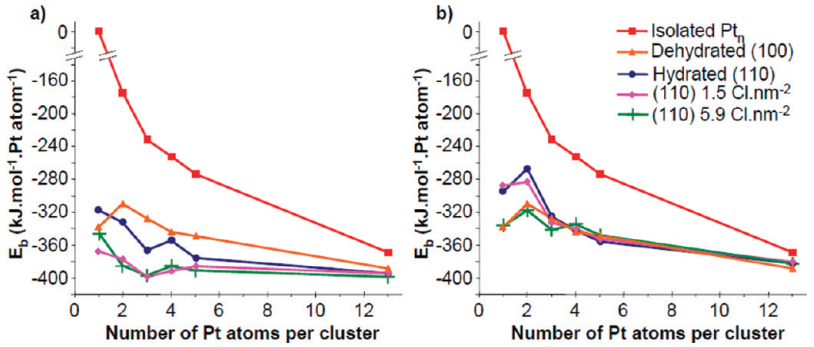

Figure 2. Binding energies for the supported and isolated Pt_n clusters as a function of the particle size for various surface terminations of the alumina support: (a) stable configurations, including potential migration of species from the support toward the cluster and (b) configurations excluding migration (note: E_b of isolated clusters and clusters on the dehydrated (100) surface do not change between a and b).

discussed in comparison with experimental data from the literature.

RESULTS AND DISCUSSION

The dehydrated (100) and partially hydrated ((110), 11.8 OH nm^{-2}) γ-Al_2O_3 surfaces are used in the continuity of ref 26 and represented in Figure 1a and b, respectively (see also the Methods section). Addressing the question of the impact of chlorine on the acidity of γ-Al_2O_3, some of us[39] studied from quantum simulations the chlorination of alumina surfaces by substituting chlorine ions for hydroxyl groups. We showed that a hydroxyl group monocoordinated to an Al atom (also labeled μ_1-OH)—in particular, Al_{IV} atoms located on the (110) surface—are preferentially substituted by Cl and we demonstrated the influence of chlorine on the hydrogen bond network between hydroxyl groups.

Chlorination of the (100) surface is not considered due to the absence of exchangeable OH groups after usual pretreatment conditions; hence, two chlorinated (110) surfaces were considered in the present work. The first one called "slightly chlorinated" contains a low chlorine coverage of 1.5 Cl nm^{-2} (Figure 1c). Assuming a specific area of 200 m^2 g^{-1} for the γ-Al_2O_3 support, as usually found for reforming catalyst,[21] and a proportion of 70 and 30% of (110) and (100) surfaces, respectively, this corresponds to an overall value of 1.7 Cl wt %, which is close to the optimal value for reforming catalysts.

The second surface contains 5.9 Cl nm^{-2} (i.e., 6−7 wt %) and is referred as the "highly chlorinated" one (Figure 1d). This surface will serve as a reference case to explore the effect of Cl coverage. Using these models, we evaluated the impact of chlorine on the metal−support interaction and on the stability of Pt_n clusters. Figure 1 summarizes also the optimal adsorption sites for Pt_n ($1 \leq n \leq 5$ and $n = 13$ respectively) with and without migration of surface species (H, OH, and Cl, which can migrate on the particle, as we show later). The tricoordinated Al_{III} atoms on the (110) surface play a major role in the case of species migration, as will be discussed later. Most labile surface species involved in migrations toward the cluster are also represented by arrows in Figure 1 (see also the Methods section).

Size Dependence for the Thermodynamic Stability of Pt_n Clusters Supported on γ-Al_2O_3 Surfaces. The adsorption of Pt_n clusters ($1 \leq n \leq 5$ and $n = 13$) on the four alumina surfaces was carried out to study their stability as a function of particle's size. The binding energies (E_b, eq 1; see Methods) corresponding to the most stable systems for each cluster size are reported in Figure 2a. Binding energies of optimal isolated Pt_n clusters (eq 2; see Methods) are also reported for comparison. The driving force for the sintering of the metallic particles is clearly illustrated here by the stronger (more negative) binding energy with increasing size. As expected, this trend is more pronounced for the isolated clusters, illustrating the stronger tendency to sinter that is expected in such a case. As a matter of reference, the most stable system is the Pt bulk with a E_b value of −511 kJ mol^{-1} (not reported in Figure 2 for the sake of clarity).

The most stable clusters on the (110) surfaces (hydroxylated, eventually chlorinated) reported in Figure 2a include migrations of surface species (OH, Cl, H) from the support toward the cluster allowing a better anchoring onto the surface, as will be detailed in the next parts. On one hand, the bond between the migrated species and the alumina surface is broken. On the other hand, this energy cost is more than compensated by the better binding between the cluster and the unsaturated surface and by the interaction between the species and the supported cluster. Hence, the Pt cluster modifies the alumina surface to improve its adhesion with the support. When an OH group (respectively Cl) migrates, the cluster induces a local dehydration (respectively, a dechlorination) of alumina. The nature of these migrations will be explained in more detail in what follows. To illustrate the impact of the migration on the stability, the binding energies of the most stable systems excluding migration are reported in Figure 2b. Note that migrations on the dehydrated (100) surface are not possible due to the absence of any labile surface groups in the experimental conditions of catalytic reforming. Therefore, the binding energy of the dehydrated (100) surface remains unchanged between parts a and b of Figure 2.

The interaction with the support strongly stabilizes the particle with respect to the isolated case. The smaller the particle, the stronger the stabilization per atom. For small particles, the adhesion on the support involves a greater fraction of the atoms, and hence, its normalized effect is simply larger. Except for an initial increase between one and two atoms, the profile excluding migration is mainly downhill with cluster size. The migration of surface species from the (110) surface to the cluster affects essentially the very small sizes and can significantly overstabilize the clusters. As a consequence, the clusters become more stable on the (110) surface of γ-alumina compared with the (100) one. More importantly, the binding energy profiles become nonmonotonic for the two chlorinated surfaces, yielding a local minimum for clusters containing three atoms. After migration, Pt_3 clusters are, indeed, more stable than clusters with 5 or 13 atoms so that sintering becomes

dx.doi.org/10.1021/cs300178y | ACS Catal. 2012, 2, 1346−1357

endothermic. This minimum is local, since the larger clusters are again favored in the limit of large size. This result demonstrates the effect of chlorine in improving the stability of small size clusters and in reducing sintering effects.

At this stage, the key result is that on hydrated and chlorinated (110) surfaces, the surface interacts even more strongly with the metallic clusters than in the case of the dehydrated (100) surface, but only upon the migration of surface species toward the cluster. The effect is enhanced by the presence of surface Cl species.

Experimentally, the influence of chlorination is already observed for chlorine content as low as 1 wt % Cl .[12,16,17] According to our results, this effect can only be explained by taking into account the migration of surface species toward the metallic phase: this is the first atomic-scale evidence elucidating the effect of chlorination observed in experiments. In what follows, we achieve a careful energetic, structural, and electronic analysis to explain the origin of the stabilization process of the Pt_n clusters on each surface.

Pt Clusters on the Dehydrated γ-Alumina (100) Surface. In the case of the dehydrated (100) surface, the formation of Pt−Al and Pt−O bonds[26] with the support strongly stabilizes the clusters (orange curves in Figure 2). The adsorption structures are illustrated in Figure 3 for Pt_1, Pt_3, and Pt_{13}.

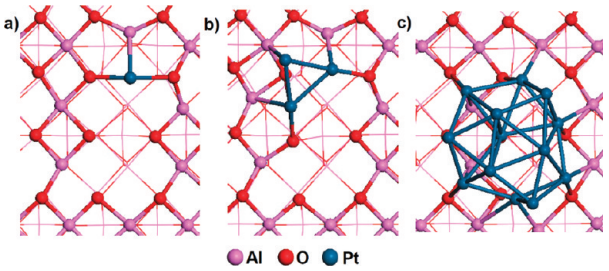

Figure 3. Top views of the most stable structures for Pt_n clusters on the (100) dehydrated surface of γ-alumina with n = (a) 1, (b) 3, and (c) 13.

The most stable geometries result from optimizing the interactions with the O and Al atoms of the support while conserving good cohesion energy between Pt atoms. The evolution of the binding energy in Figure 2 shows a maximum for Pt_2 before decreasing continuously, in agreement with Mei et al.[40] The single atom Pt_1 is a metastable state, implying an associated barrier for the nucleation of Pt_2.

The comparison with the interaction of Pt_1 on the dehydrated (0001) α-Al_2O_3 surface reveals that less exoenergetic values (close to −200 kJ mol^{-1}) are generally found on α-Al_2O_3.[28,31,32] This may be explained by the higher coordination of Al and O surface atoms and, thus, a lower intrinsic surface reactivity. A similar behavior is observed by Nasluzov et al.[33] for Pt_3 in an upright configuration on a dehydrated (0001) α-Al_2O_3 surface with a binding energy close to −250 kJ mol^{-1}, whereas we found a value of −328 kJ mol^{-1} for a configuration in which Pt_3 is oriented parallel to the surface (the perpendicular mode in our model leads to less stable systems). This effect is thus driven by the accessibility of Al atoms on γ-alumina, which explains its superior ability to stabilize highly dispersed transition metal clusters.

It can be noticed that for Pd_n clusters[36] on the same surface, the binding energies were found smaller (between −166 and −220 kJ mol^{-1}) than for Pt_n, which can be explained by the less diffuse 4d orbitals (versus 5d for Pt), leading to weaker interactions of Pd atoms with their neighbors (Pd, Al, or O). The stronger Pt−support interaction may also explain why it is experimentally easier to synthesize highly dispersed Pt particles than Pd ones.

Pt clusters on the Hydrated and Chlorinated γ-Alumina (110) Surface without Migration of Surface Species. Examples of optimal structures of Pt_1 and Pt_3 clusters on the hydrated and chlorinated γ-alumina (110) surfaces, without migrations of surface species toward the cluster, are shown in Figure 4a−c and 5a−c (equivalent structures for Pt_{13} are shown in Supporting Information S3). Compared with the case of the dehydrated (100) surface, the geometry of the adsorbed clusters is generally closer to that of the gas phase due to weaker cluster−surface interaction and cluster or surface deformation, as shown for Pt_{13} in ref 26.

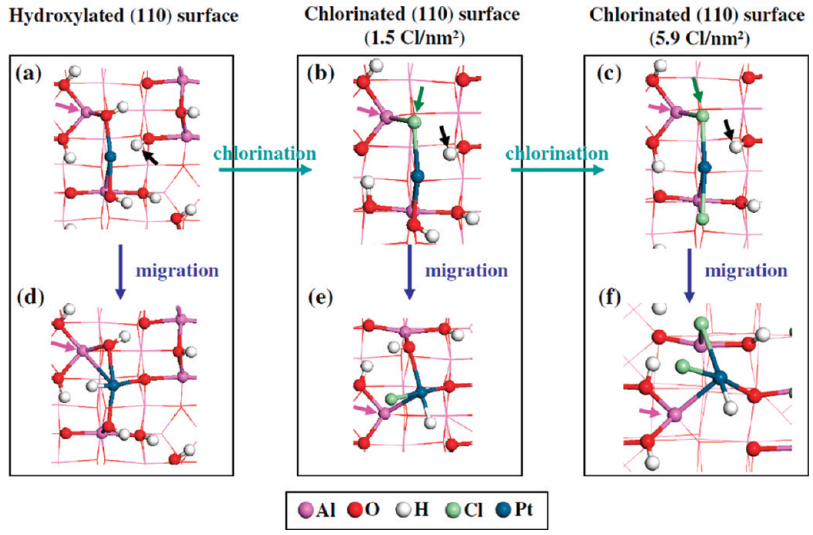

Figure 4. Top views (except f: perspective view) of the optimal structures for the Pt_1 cluster on the hydrated and chlorinated (110) surfaces of γ-alumina. (a−c) Excluding migration of surface species and (d−f) including migration toward the cluster of (d) one H, (e) 1 H + 1 Cl, and (f) 1 H + 1 Cl. Pink, green, and black arrows mark the Al_{III} atom and the OH, Cl, and H species involved in the migration, respectively.

dx.doi.org/10.1021/cs300178y | ACS Catal. 2012, 2, 1346−1357

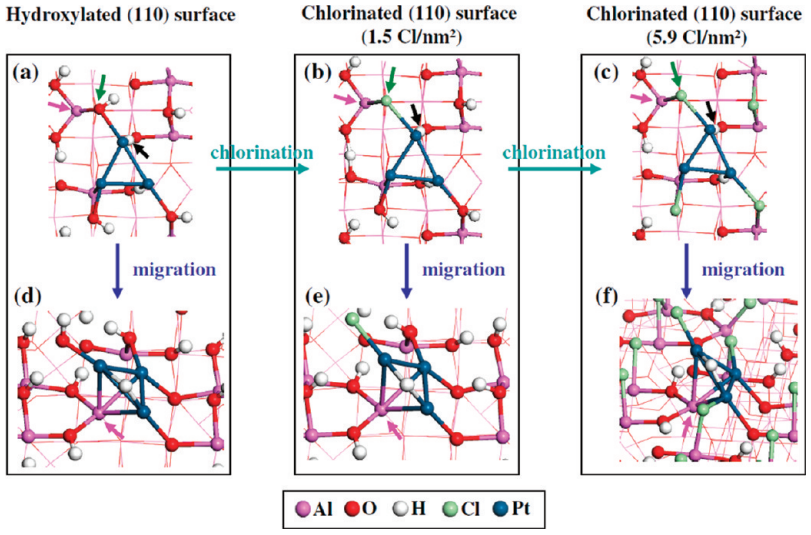

Figure 5. Top (a–c) and perspective (d–f) views of the optimal structures for the Pt_3 cluster on the hydrated and chlorinated (110) surfaces of γ-alumina. (a–c) Excluding migration of surface species and (d–f) including migration toward the cluster of (d) 1 H + 1 OH, (e) 1 H + 1 Cl, (f) 1 H + 1 Cl. Pink, green, and black arrows mark the Al_{III} atom and the OH, Cl, and H speices involved in the migration, respectively.

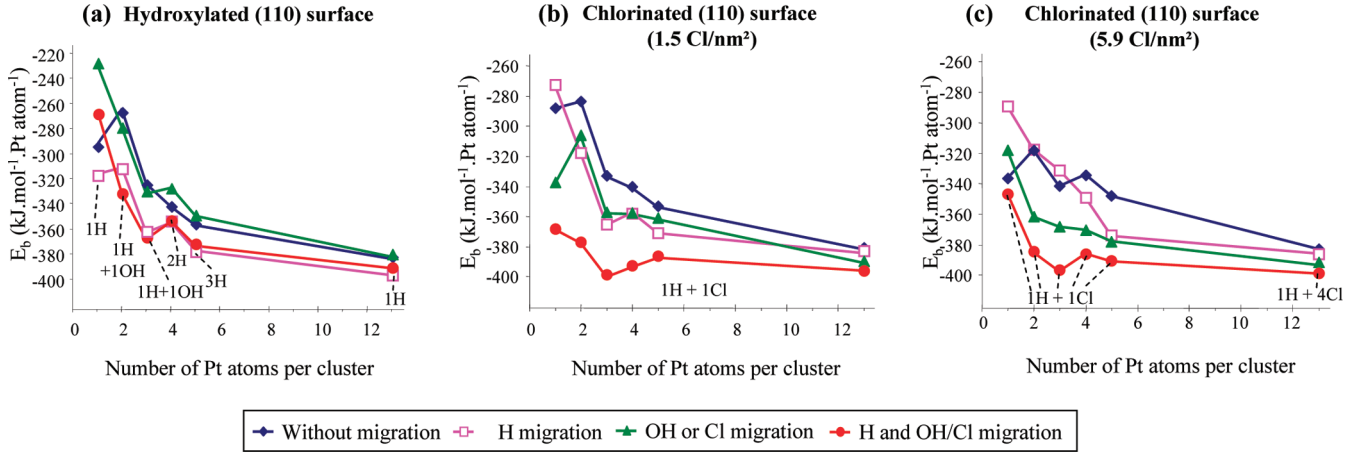

Figure 6. Binding energies of Pt_n clusters on the hydrated and chlorinated (110) γ-Al_2O_3 surface as a function of cluster size, including the migration of surface species toward the cluster. The optimal number of migrated species is also given.

The surface with low chlorine content (1.5 Cl nm^{-2}) exhibits cluster binding energies close to the hydrated (110) surface (Figure 2b) in the absence of migration phenomena. By contrast, the surface with a high chlorine content (5.9 Cl nm^{-2}) induces a stronger stabilization of small Pt clusters (n = 1–3, green curve in Figure 2b). Since the adsorption configurations are very similar to those found on a hydrated (110) surface for the two chlorinated surfaces, the intrinsic reactivity of chlorine sites must be invoked to justify this enhancement. At this stage, we must recall that the stability of adsorbed OH groups was stronger than most of the Cl species (except for Al_{III}–Cl), as revealed by our earlier study.[39] This induces a metastable character of the γ-alumina surface at high chlorination degree. The chlorinated surface thus interacts more strongly with Pt clusters. We will also show later that the Pt–Cl interaction is stronger than the Pt–OH interaction. Thus, the cluster binding energy calculated on the highly chlorinated surface is as strong as or even stronger than the one obtained on the dehydrated (100) surface. This trend appears to be the first consequence of the chlorination, which increases the reactivity of the surface and, thus, increases the stability of the supported Pt_{1-3} clusters.

Note that the comparison with Pd_n clusters adsorbed on the hydrated (110) surface without any migration[36] follows the same trends as previously discussed on the (100) surface. The binding energies are stronger for Pt, and a different local minimum is found (Pt_1 instead of Pd_2). This highlights again the different strength of metal–support interaction for the two metals.

Pt Clusters on the Hydrated and Chlorinated γ-Alumina (110) Surface with Migration of H Atoms. The migration of H atoms from surface hydroxyl groups located on the hydrated (110) alumina surface (shows as black arrows in Figure 1b), to the metallic particles results in a stabilization of the system compared with the adsorption without migration (Figure 6a; see also the structures in Figure 4d and Supporting Information S3). This is due to the combined effect of (i) the affinity between the migrated H atoms and small Pt_n clusters[41] and (ii) the new interaction between the Pt_n cluster and the deprotonated O atom belonging to the OH group involved in H migration. This trend is particularly true for the smallest clusters. This second parameter explains why protons

dx.doi.org/10.1021/cs300178y | ACS Catal. 2012, 2, 1346–1357

preferentially come from OH groups in close vicinity of the adsorbed cluster (Figure 1b).

As a consequence of the creation of new Pt−O bonds, combined with the amount of H atoms hosted on small clusters, the optimal numbers of migrated H atoms are one for Pt_1 and Pt_2, two for Pt_3 and Pt_4, and three for Pt_5. One migrated H atom is also found for Pt_{13} as being the most stable: the energy is very close to the two migrated H atoms, as found in our previous work.[26] The small number of H atoms per surface Pt involved in reverse spillover observed for clusters such as Pt_{13} is likely due to the reduced structural deformation capability. Indeed, significant cluster deformation is required to interact with several O atoms coming from OH groups. The total energy stabilization associated with H migration is $n\Delta E_b$, where n is the number of platinum atoms. It varies in a nonmonotonic way between −23 kJ mol^{-1} for Pt_1 and −156 kJ mol^{-1} for Pt_{13}.

Previous theoretical studies showed that the migration of one H atom from a surface hydroxyl group stabilizes a single Pt atom on hydrated (0001) α-Al_2O_3.[29,31] The stabilization values of −29 and −27 kJ mol^{-1} obtained by Briquet et al.[29] and Xiao and Schneider,[31] respectively, are comparable with our value of −23 kJ mol^{-1}. Note that in our earlier work,[26] the position of the Pt_{13} cluster was kept identical to the most stable one found without migration, yielding a binding energy stabilization due to H migration of −5 kJ mol^{-1} per Pt atom (total stabilization of −65 kJ per mole of cluster). A more stable situation was found in the present work by shifting the cluster to a new location in the vicinity of the O atoms from the OH groups involved in the H migration and also in the vicinity of the Al_{III} atom (see additional explanations in the Supporting Information, S3). This allows the cluster to interact with the support through Pt−O bonds; hence, stabilizing the system.

On the slightly chlorinated (110) surface, the most stable adsorption geometries for clusters after H migration are obtained by the interaction of Pt with the O atoms of the OH groups having transferred their proton. However, contrary to the hydroxylated surface, the migration of H atoms is not always a factor of stabilization (Figure 6b, c), in particular, for Pt_1. Actually, the Pt−O distance (where O is the deprotonated atom), increases from 2.36 (hydroxylated surface) Å to 2.52 Å (slightly chlorinated surface). This is due to the fact that the Cl atom interacting with Pt_1 exhibits a distance to Al that is longer than the Al−OH bond before Cl substitution. Hence, Pt_1 is shifted away from the surface, which reduces its interaction with the alumina surface. This phenomenon is even reinforced on the highly chlorinated surface because two Cl atoms (instead of one) are interacting with Pt_1, which is pushed even farther from the surface: the Pt−O distance growths to 2.78 Å .

Pt Clusters on the γ-Alumina (110) Surface with Migration of OH or Cl Groups. The migration of one OH or Cl group from the alumina surface toward the platinum clusters allows the clusters to interact with the coordinatively unsaturated Al Lewis acid site originally bonded to the OH/Cl group. The stronger Lewis acidic site is the Al_{III} atom (pink arrow in Figure 1b−d). The associated μ_1-OH or Cl group (green arrow in Figure 1b−d), despite its strong interaction with the Al_{III} atom, is found to be the most prone to migration. To stabilize the system, the energy loss induced by the departure of the OH or Cl group must be compensated by new Pt−Al interactions.

In the case of OH migration on the hydroxylated surface, the most stable systems found often exhibit hydrogen bonding between the migrated OH and nearby surface hydroxyls. The stabilizing impact of OH migration on the binding energy is far less pronounced than the one of H migration (Figure 6a). At best, only one OH group can migrate for each studied cluster. The migration slightly stabilizes Pt_2 and Pt_3 but slightly destabilizes Pt_4, Pt_5, and Pt_{13} compared with the absence of migration. By contrast, the OH migration on Pt_1 strongly destabilizes the system (+61 kJ mol^{-1}), a part of it being assigned to the lack of hydrogen bond between the Pt−OH group and other hydroxyls on alumina (see Supporting Information S4 for a more detailed explanation).

This destabilization trend differs from the observations by Xiao and Schneider[31] on the hydrated α-Al_2O_3 (0001) surface, where the migration of hydroxyl group weakly stabilizes the adsorption of Pt_1. This different trend is mainly explained by the different hydroxyl contents found on the two supports models: it is lower on the hydrated γ-Al_2O_3 (110) surface than on the hydrated α-Al_2O_3 (0001) surface. On γ-Al_2O_3 (110), following the analysis reported in Supporting Information S4, the migrated OH group cannot be stabilized by the formation of hydrogen bonds with a nearby hydroxyl group, whereas this H-bonding is possible on the α-Al_2O_3 (0001) surface. In addition, the lower hydroxyl content of γ-alumina enables the stabilization of Pt_1 without any OH migration, being inserted in a bridging position between one Al atom and two OH groups (Figure 4a): this situation is possible on hydroxylated α-alumina only after OH migration. Finally, the different nature of the alumina polymorph infers a lower coordination for some Al atoms on the γ-Al_2O_3 surface. Thus, the migration might also be constrained by the higher stability of the Al_{III}−OH bond on γ-Al_2O_3.

By contrast, the migration of one chlorine atom from the alumina support to the cluster is overall stabilizing on both chlorinated surfaces (see green curves in Figures 6b, c) up to 50 kJ mol^{-1} per Pt atom. Top and bridge sites are the most stable adsorption sites of chlorine on Pt_n clusters, depending on the particle's morphology and size (bridge adsorption sites were found most stable for palladium clusters[42]). On the slightly chlorinated (110) surface, this stabilization occurs for every particle size studied, in particular, for Pt_{13}, with an energy gain of −9 kJ mol^{-1} per Pt atom (i.e., a total stabilization of −117 kJ mol^{-1}). Regarding the highly chlorinated surface (green curve in Figure 6c), the single exception is Pt_1 (+18 kJ mol^{-1}). In particular, for Pt_3, a gain in stability of −26 kJ mol^{-1} per Pt atom is calculated. The stabilization is generally higher than on the slightly chlorinated (110) surface for similar adsorption structures.

The binding energy is significantly lower (more exothermic adsorption) than on the hydroxylated surface (particularly for Pt_1). Comparing the local structures of Pt_1 and Pt_3 after OH and Cl migrations (Pt−Al and Pt−O bond distances), we did not notice significant differences; hence, the enhanced exothermicity cannot be explained by these structural parameters. To carefully explain this trend, we made a detailed energy decomposition. We propose to come back to this discussion in the forthcoming paragraphs ("energy decomposition").

Pt Clusters on the γ-Alumina (110) Surface with Simultaneous Migration of H Atoms with OH or Cl Species. To our knowledge, the simultaneous migration of H with OH or Cl species has never been considered. With the exception of Pt_1 on the hydroxylated surface, the simultaneous migration of H with OH or Cl species always results in a

dx.doi.org/10.1021/cs300178y | ACS Catal. 2012, 2, 1346−1357

stabilization of the systems with respect to the nonmigration cases (Figure 6).

On the hydroxylated surface, for most cluster sizes, the H migration bears the major energy gain (see also Supporting Information Table S1). For the Pt_2 and Pt_3 clusters only, one (H + OH) migration is slightly more stable than the H migration. This slight energy gain can be assigned to the favorable bonding with three surface sites: the Al_{III} and the two nearby O atoms located in the pink disk in Figure 1b. The adsorption of Pt_3 on the surface always favors the formation of a Pt_3 triangle with each Pt atom involved in one Pt−Al_{III} bond (Figure 5d).

On the chlorinated surfaces, the simultaneous migrations of H and Cl atoms is significantly more favorable than Cl migration alone, and it gives the most stable structures for all cluster sizes on both chlorinated surfaces. In several cases, a synergy effect is observed between Cl and H migration because a stronger energy gain is obtained for the simultaneous (H, Cl) migrations than the cumulated energy gains for Cl and H migration alone. For Pt_n clusters ($1 \leq n \leq 3$), each Pt atom interacts with the Al_{III} atom (see Figures 4e, f, 5e, f). In the case of larger clusters such as Pt_{13}, only two Pt atoms are directly bonded to the Al_{III} site (see Supporting Information S3). This trend is also true for the hydroxylated surface. This explains the relatively larger stabilization effect of H + Cl migration for the smallest clusters as compared with bigger ones. The stabilization effect of (H + Cl) migration is quantitatively very similar on both chlorinated (110) surfaces. This reveals that the stabilization observed after the chlorination treatment is already effective for the lowest chlorine content used in reforming catalysts.

It is worth noting that for Pt_4 and Pt_5, flat clusters are more stable than 3D morphologies, in contrast with systems excluding migration. The migration of a single H and a single Cl atom facilitates the access of metal atoms to the alumina surface and induces a maximization of the metal−support interaction with the Al_{III} and oxygen atoms, thus leading to more stable systems after cluster flattening. Note also that for the Pt_{13} cluster adsorbed on the highly chlorinated surface, the most stable geometry (taking into account H and Cl migrations) was investigated by molecular dynamics, leading to a flattening of the cluster and strong interaction of the support due to the migration of several surface groups. The approach and the results are detailed in Supporting Information S5.

Energy Decomposition: Origin of the Stabilization of Subnanometer Clusters on Chlorinated Surfaces. The calculations reveal more exothermic binding energies for the migration of H and Cl on the chlorinated (110) surface than in the case of the simultaneous migration of H and OH groups on the hydrated surface: this is a strong evidence of the impact of chlorination on the stability of small Pt_n clusters. Moreover, a peculiar stability of supported Pt_3 clusters on chlorinated surfaces appears after migration of surface species (in particular, Cl and H). To explain these striking results, we have undertaken a detailed analysis with a decomposition of the energy. For that, we chose three relevant cluster sizes: Pt_1, Pt_3, and Pt_{13} clusters. An analysis for isolated clusters (Supporting Information S6) reveals that the interaction energy of Pt_n clusters with dissociated HCl species is significantly stronger than with the dissociated H_2O molecule, by more than 80 kJ mol^{-1}. This suggests that intrinsically, the higher affinity of platinum for H + Cl compared with H + OH is one of the driving forces of the effect of chlorine.

Then, we considered H + X migration on the hydrated (X = OH) and the slightly chlorinated (X = Cl) (110) surfaces. We decomposed the binding energy, E_b, into three terms, as shown in Figure 7. The first term ($\Delta_r U_1$) represents the energy cost

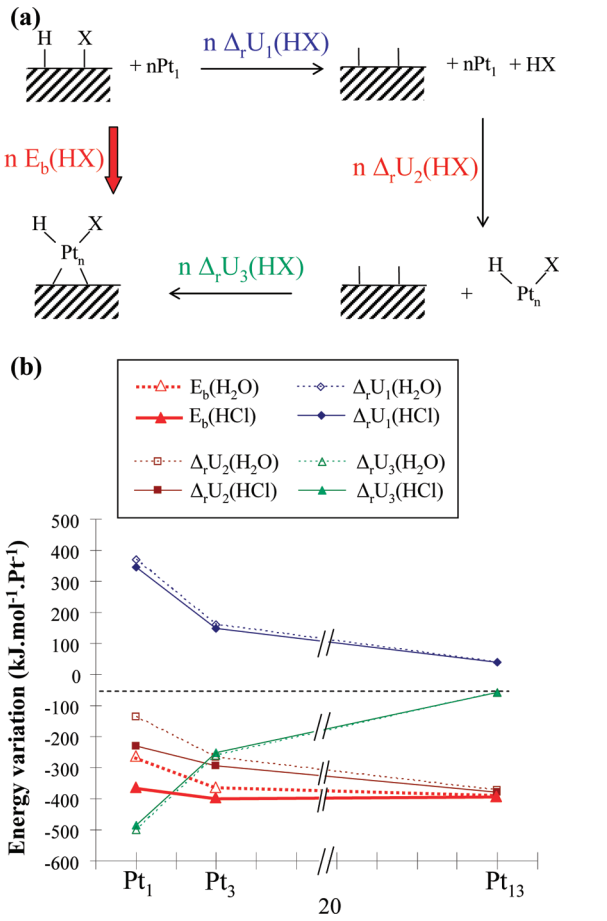

Figure 7. Decomposition of the binding energy of the adsorbed Pt_n cluster on which a H + X (X = OH or Cl) pair has migrated. (a) Born−Haber cycle used for the decomposition and definition of energy terms and (b) values calculated for Pt_1, Pt_3, and Pt_{13} clusters on the hydrated (H + OH) and slightly chlorinated (H + Cl) surface.

for the loss of the H−X pair from the support, that is, the inverse of the affinity of H−X for the support. The second term ($\Delta_r U_2$) contains two contributions: the binding energy of the isolated Pt_n cluster and the adsorption energy of the HX molecule on the isolated Pt_n (in a similar geometry as in the adsorbed state). The third term ($\Delta_r U_3$) quantifies the interaction of the {X−Pt_n−H} fragment with the surface. Figure 7b depicts the values of each term for both surfaces and for the three clusters sizes considered.

It appears that the $\Delta_r U_1$ and $\Delta_r U_3$ terms are not significantly different from H_2O to HCl. On the contrary, the $\Delta_r U_2$ term is determining. The interaction of HCl with Pt_n contributes an additional 75−95 kJ/mole of cluster to the stabilizing effect with respect to the interaction of H_2O (differences are more apparent for the smallest clusters in Figure 7 because of the normalization by n). It is interesting to recall that the stronger bond strength of chlorine compared with oxygenate ligand was also calculated for Pt mononuclear species.[43] This contribution

dx.doi.org/10.1021/cs300178y | ACS Catal. 2012, 2, 1346−1357

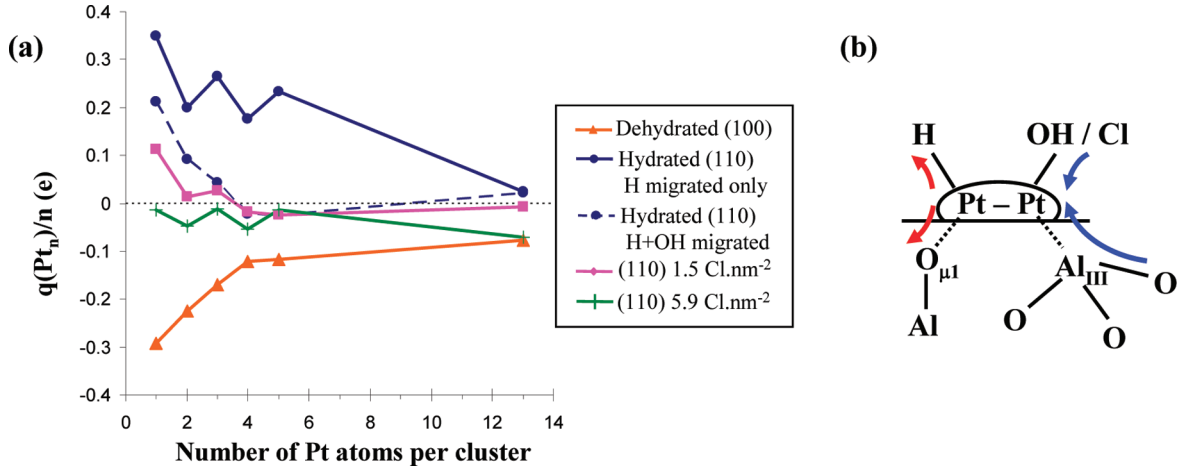

Figure 8. (a) Bader charge analysis of the supported Pt_n clusters (mean charge per Pt atom) as a function of sizes. For the chorinated surfaces, the most stable configurations are reported (including migration of Cl and H species); for the hydrated surface, two competitive configurations are reported. Note: a negative (respectively, positive) value means anionic (respectively, cationic) species. (b) Schematic description of the charge transfers induced by migration of surface species toward the Pt clusters. Electron donations to the cluster are in blue, and electron withdrawing is in red.

is the main explanation for the specific behavior of chlorine migration.

In addition, Figure 7b shows that the metal−support interaction energy counterbalances the energy loss induced by the HCl departure from the surface and by the surface relaxation. The metal−support interaction ($\Delta_r U_3$) is predominant for very small clusters ($n \leq 3$) interacting with three surface sites: 1 Al_{III} and 2 O atoms invoved in the migration of the H and Cl atoms. For a larger cluster, such as Pt_{13}, the stabilizing factor results mainly from the contribution of the cluster binding energy in $\Delta_r U_2$. For Pt_3, the metal−support interaction energy $\Delta_r U_3$ is close to the $\Delta_r U_2$ contribution. There is thus a compensation effect that is at the origin of the minimal binding energy found for Pt_3 supported on chlorinated surfaces.

Structural Analysis and Comparison with Experimental Results. Interatomic distances are cluster size and surface-dependent (Table S2 in the Supporting Information). The mean Pt−Pt distance generally increases from Pt_2 to Pt_{13} (from 2.52 to 2.67 Å). This is a well-known behavior for small clusters[24,36,44−47] and the associated low coordination metal atoms. Migration of surface species on the smallest clusters induces some variations to this rule: for example, the Pt−Pt distance in the Pt_2 cluster increases from 2.46 Å without migration to 2.56 Å after migration of 1 H and 1 Cl on the slightly chlorinated surface. Migrating groups thus tend to expand the clusters, which is consistent with the effects of adsorbates (in particular, hydrogen[41,45,48]).

Pt−Cl distances after migration of chlorine on clusters are mostly measured around 2.3 Å, which is consistent with experimental evaluations by EXAFS.[16,19] Note that these experimental measurements were performed on samples exhibiting oxidized forms of platinum, whereas no Pt−Cl bonds were ever observed on reduced samples. This could be due to the lack of sensitivity of the technique regarding the small number of Cl atoms per Pt in the systems, which is consistent with our prediction for Pt_n clusters with $n \geq 3$ of mean Pt−Cl coordination number as low as 0.1−0.3 per platinum. For Pt_1 and Pt_2 on the highly chlorinated surface, mean Pt−Cl bonds reached 2.5 Å as a result of the existence of Cl atoms located at around 2.6−2.7 Å in addition to smaller distances with migrating Cl groups (2.3 Å).

Pt−O distances are generally measured around 2.1−2.3 Å, in line with experiments.[24] Some very short distances (2.05 and 2.02 Å) are measured for Pt_1 and Pt_2 clusters on the dehydrated (100) surface. This can be explained by the interstitial hole located on the (100) surface, which favors the stabilization of the Pt_1 (Figure 3a) and Pt_2 clusters (to a lower extent).[36] When the cluster's size increases, the Pt atom initially located in this hole is extracted to establish the Pt−Pt interactions. Hence, for larger clusters, the interfacial Pt atoms prefer to interact with more numerous—even if more distant—atoms of the surface.

A final structural analysis can be made on the Pt−Al bonds revealed by our calculations. According to EXAFS experiments,[24] it was proposed that the insertion of H atoms at the metal−support interface may explain the observation of longer Pt−O distances, in particular, after reduction at 573 K (d_{Pt-O} = 2.66 Å). Our calculations on chlorinated systems do not reveal such "long" Pt−O distances. As already discussed in our previous work for Pt_{13} on a nonchlorinated surface,[41] our models studied here in the presence of Cl confirm the presence of Pt−Al bonds with distances varying between 2.3 and 2.7 Å, which may also account for the long metal−support distance suggested by Vaarkamp et al.[41] In addition, we show that some Pt−Cl distances can reach 2.6−2.7 Å for very small clusters (see previously, Pt_1 and Pt_2) on the highly chlorinated surface. They are not the migrating Cl atoms, which are closer to the Cl atoms, but additional Cl atoms. Thus, we can assign the "long" Pt−X distance either to X = Al, or X = Cl.

Interestingly, we notice that Pt_3 clusters were also observed by experimental Z-STEM analysis on γ-Al_2O_3.[22,49,50] According to the preparation process, the presence of residual chlorine atoms on the surface cannot be excluded. Finally, Stakheev et al.[47] showed by EXAFS that the particles tend to flatten upon chlorination of the alumina support. From our work, we can assign this observation to the improved metal−support interaction due to migration of H and Cl species from the support to the particle, with enhanced formation of Pt−O and Pt−Al bonds. Our calculations also recover this behavior for Pt_4 and Pt_5 as aforementioned.

dx.doi.org/10.1021/cs300178y | ACS Catal. 2012, 2, 1346−1357

Electronic Analysis. The atomic charge was evaluated with the Bader approach on the most stable systems with and without migration. The results for the most stable clusters, regarding the Pt_n moieties, are reported in Figure 8a. Extended results are reported in Supporting Information S7, as a function of H, OH, or Cl and H + OH or H + Cl migrations, and for various components of the system (Pt_n, H, OH, Cl species).

On the dehydrated (100) surface, the Pt_n clusters are negatively charged (from −0.29 to −0.08 *e*/Pt atom), in line with previous theoretical suggestions.[26,28,29] In a previous work,[26] we showed for Pt_{13} that this charge transfer from the support corresponds to an electron transfer from O atoms to Pt through Al atoms interacting with Pt clusters.

On the hydrated and the chlorinated (110) surfaces, the electrostatic charge of the Pt_n cluster directly depends on the migration involved. Without migration (Supporting Information S7.1), the hydroxyl or chlorine interface reduces the charge transfer via the Al atoms, as previously described for the dehydrated (100) surface. The H migration favors the Pt−O interaction, leading to an oxidized state of the Pt clusters bearing a positive charge. Migrated H atoms adsorbed on the clusters are generally rather neutral (Supporting Information S7.2) and are thus not negatively charged (no hydride nature). As a matter of reference, the mean charge of protons located on the OH species of the surface not in interaction with the cluster is +0.67*e*. Hence, Pt clusters are electronically depleted by the σ Pt−O bond formation allowed by the migrated H protons, which simultaneously gains electrons. Single migrations of OH or Cl from (110) surfaces to the Pt_n clusters induce opposite effects: the charge of the cluster gets more negative, since migration favors the Pt−Al interaction responsible for the transfer of electrons toward the Pt cluster. The resulting charge of the clusters is then closer to the values found on the dehydrated (100) surface (Supporting Information S7.3).

The increased electronic population on the Pt_n cluster is accompanied by a reduced charge on the OH or Cl fragments. Pt clusters are thus clearly enriched in electrons due to charge transfers from both Al surface atoms and migrated OH or Cl species. As a global result, the most stable clusters on each surface exhibit the charge depicted in Figure 8a. They are negatively charged on the (100) surface, whereas on the hydrated (110) surface, they are positively charged when only H migration occurs. However, the simultaneous (H + OH or H + Cl) migrations reveal a compensating effect on the cluster electronic population. This charge compensation of effects implies that the charge of Pt_n is more or less neutral, particularly in the case of the chlorinated surfaces. These variations of the electronic population of the particle as a function of the acidity of the support will clearly have an incidence on the reactivity of the metallic aggregates. The counterbalancing contributions of the different atoms and species interacting with Pt_n clusters are summarized and schematized in Figure 8b, illustrating the various charge flows.

Considering (Pt_n + H + OH or Pt_n + H + Cl) fragments formed after migration, their overall electronic charges are negative (Figure 9) and increase (decrease in absolute value) with the particle size (when normalized per Pt atom). As a consequence, the hydrated and chlorinated surfaces become positively charged, which confirms that the overall electron transfer occurs from the surface to the fragment. Interestingly, the variation of the (Pt_n + H + OH or Pt_n + H + Cl) charges as a function of size follow a very similar quantitative trend for all systems, including the dehydrated (100) surface, especially for small sizes ($n \leq 5$). This is a manifestation of the intrinsic property of alumina regarding the metal/support interaction, independently of the surface groups present.

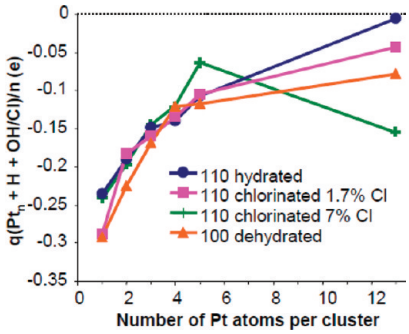

Figure 9. Bader charge analysis of the supported (Pt_n + migrated species) fragment normalized by the number of Pt atoms (mean charge per Pt atom) with simultaneous migrations of (H and OH) or (H and Cl). OH migrations are considered for the hydrated surface and Cl migration for the chlorinated ones. The (100) surface is recalled for comparison, even if no migration obviously occurs.

We finally performed density of states (DOS) analysis for the Pt_3 system supported on the (110) alumina surface, either hydrated (H and OH migration) or slightly chlorinated (H and Cl migration). These systems are those considered for the energy decomposition (Figure 7). Figure 10 depicts the DOS projected on the platinum atom bearing the migrated OH or Cl species, as well as projections on migrated species themselves.

Figure 10 shows the overlap between Pt orbitals (essentially of d character for energies higher than −8 eV) and p orbitals of O or Cl atoms. However, the Cl p orbitals are higher in energy, and they reveal a better mixing with the Pt d orbitals in the region [−4 eV, 0 eV], whereas a nonnegligible contribution of O p states is localized at the bottom of the d band. Thus, the orbital interaction is, hence, more favorable for Cl. This corroborates the stronger affinity of Pt for Cl rather than for OH and helps to rationalize the higher stability of Pt_n clusters on the chlorinated surface than on the hydrated one once migration of H and Cl is taken into account.

CONCLUSIONS

The structural, stability, and electronic properties of platinum clusters containing 1−5 and 13 atoms deposited on the (100) and (110) γ-Al_2O_3 surfaces were investigated by periodic density functional theory calculations. The surface state of the alumina support (dehydrated (100) surface, hydrated, and chlorinated (110) surfaces) was taken into account to elucidate its effect on the stability of the metallic phase. Calculations demonstrate a strong influence of surface species' rearrangement to stabilize Pt clusters. The migration phenomenon of surface species (H, OH, Cl) toward Pt clusters is shown as a key factor to stabilize subnanometer size clusters on alumina.

This effect is particularly strong in the case of chlorinated surfaces where simultaneous migration of chlorine and proton drastically impacts the clusters' binding energy. After Cl and H migration on the particle, the stability of Pt_n clusters on the chlorinated (110) surface is higher than that on the hydrated (110) surface. An energy decomposition scheme highlights that the gain from increased metal−support interaction energy is larger than the cost to detach the chlorine and proton from the surface. This stabilization is mainly explained by the anchoring of the clusters to the surface by the formation of Pt−O and Pt−

dx.doi.org/10.1021/cs300178y | *ACS Catal.* 2012, 2, 1346−1357

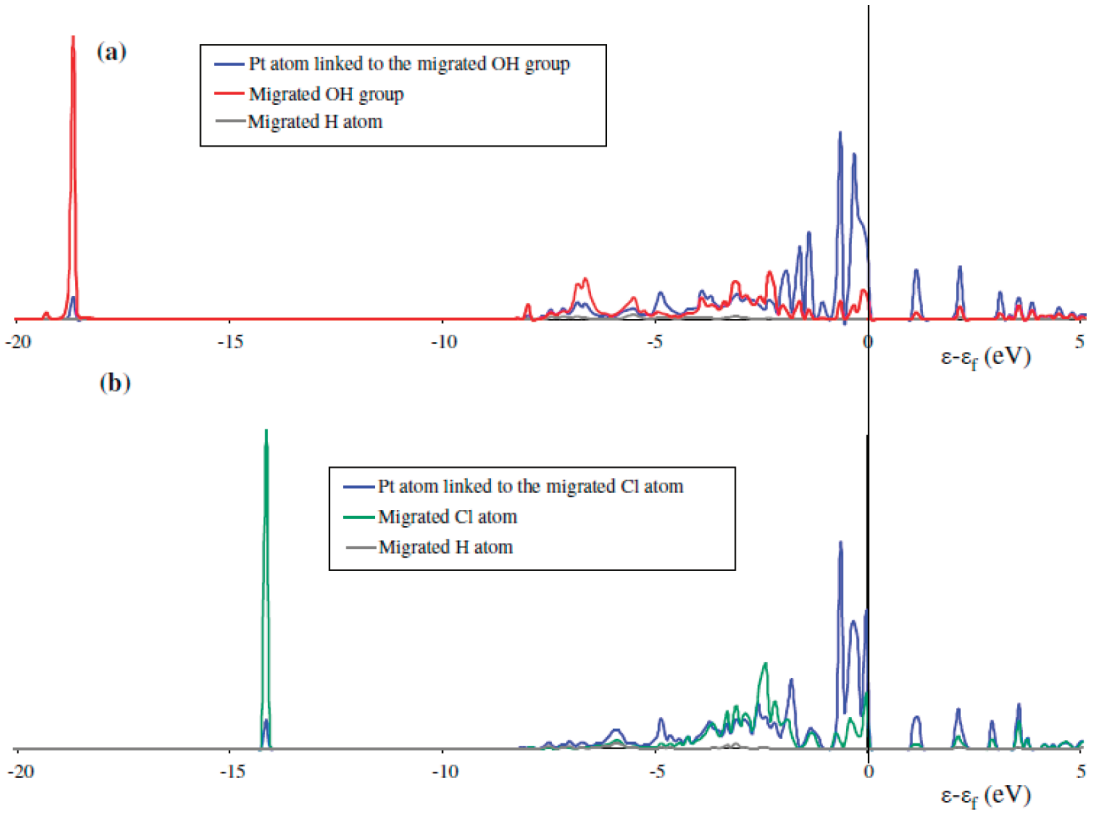

Figure 10. Density of states projected on the Pt atom bearing the migrated OH or Cl group and on migrated species for the Pt_3 clusters supported on γ-Al_2O_3(110) with H + X migration. (a) X = OH, hydrated surface, and (b) X = Cl, slightly chlorinated surface. The energy is referenced to the Fermi level.

Al_{III} bonds. OH and Cl species stabilize the low coordinated Al_{III} on the (110) Al_2O_3 surface, temporarily passivating it, but the small clusters are able to displace these "protecting groups" to establish a strong bond with Al_{III}. Moreover, the platinum−chlorine interaction energy is stronger than the platinum−hydroxyl interaction energy. As a consequence, chlorine acts as a capping surface ligand, which is at the origin of a greater stabilization of small Pt clusters on the chlorinated (110) surfaces.

The role of chlorine to limit the sintering of metallic particles is thus rationalized: chlorination is therefore of prior interest for the stabilization of highly dispersed catalysts. Indeed, on chlorinated surfaces, Pt_3 is found as a local minimum for the binding energy; thus, the sintering into larger particles would require overcoming a significant activation barrier (Pt_3 being more stable than Pt_{13} on this surface).

These results shed new light on the impact of chlorine acting as a surface ligand, thus limiting the sintering of the metallic phase and helping for its optimal dispersion. This phenomenon was empirically invoked in previous experimental works,[16,17] reporting the drastic impact of chlorine loading on Pt dispersion. Moreover, we show that the chlorinated alumina (110) surface can thus be considered as a "reservoir" of small Pt clusters anchored on the Al_{III} site.

Chlorination is also shown to impact the electronic state of the particle, which can be expected to modulate its reactivity. However, the question of the accessibility of the "chlorine-capped" platinum atoms remains open.[18,19] The operating conditions (O_2 or H_2 atmospheres) could further tune this accessibility.

METHODS

Total Energy Calculations. Periodic DFT calculations were carried out with the PW91[51] exchange-correlation functional as implemented in VASP 4.6.[52,53] The projector-augmented wave (PAW)[54] method was used to describe the electron−nuclei interactions. The one-electron functions were developed on a basis set of plane waves that was limited to a cutoff energy of 400 eV. Spin-polarized calculations were performed with the interpolation formula of Vosko, Wilk, and Nusair.[55] Partial occupancies were determined with a Gaussian smearing with a width of 0.02 eV. Atomic charges were calculated by Bader charge analysis.[56]

Models. Regarding the bulk structure of γ-alumina, former theoretical studies based on DFT calculations showed that a model with occupied nonspinel sites is the most stable structure.[57−59] Moreover, some of us[37,38,60−63] established the evolution of the hydroxyl (OH) coverage as a function of pretreatment temperature for the most representative alumina (100) and (110) surfaces (accounting for 90% of the exposed surface area of alumina samples[15]) and validated the model from the simulation of the infrared spectra or of the adsorption of probe molecules. We also showed that after a high temperature pretreatment (above 600 K), the (100) surface is totally dehydrated, whereas the (110) surface is still partially hydrated, notably due to its highly reactive Al_{III} sites.[37,38,62]

The corresponding dehydrated (100) and partially hydrated ((110), 11.8 OH nm^{-2}) γ-Al_2O_3 surfaces are used in the continuity of ref 26 and represented in Figure 1a and b, respectively. All γ-Al_2O_3 surfaces (including the chlorinated one) were modeled by four alumina layers separated by vacuum

dx.doi.org/10.1021/cs300178y | ACS Catal. 2012, 2, 1346−1357

thicknesses of 15.5−18.5, depending on the surface, which ensures a good convergence of binding energies. Compared with previous works,[37,38] a (3 × 2) and a (2 × 2) supercell (with respect to the irreducible unit cell) were used to model the adsorption of Pt_n clusters on the (100) and the (110) surfaces respectively (Figure 1a, b). This corresponds to surface cells of 16.14 × 16.78 Å^2 and 16.71 × 16.78 Å^2, respectively. The supercell of the hydrated surface was also used for the chlorinated ones. Because of the large size of the unit cell, calculations were performed at the Γ point. The platinum clusters were adsorbed on the top side of the alumina slab, and a dipolar correction was applied to remove the spurious interaction of surface dipoles between slabs. The two bottom alumina layers were fixed, and the rest of the system was optimized until the forces were lower than 0.05 eV Å^{-1}, which was found to provide satisfactory accuracy on binding energy and geometries.

Energetic Analysis. To analyze the evolution of the stability of the clusters on each of the four surfaces, the normalized cluster binding energy, E_b, in the presence of the surface was calculated, with the isolated Pt atoms and the bare surface as a reference, following eq 1:

$$E_b = \frac{1}{n}\left(E_{Pt_n/Surf} - E_{Surf} - nE_{Pt_1}\right) \quad (1)$$

where n is the number of Pt atoms per cluster, $E_{Pt_n/Surf}$ is the energy of the Pt_n cluster supported on the various surfaces, either dehydrated (100) or hydrated (110) or slightly or highly chlorinated (110). E_{Surf} is the energy of the bare surface and E_{Pt_1} is the energy of one isolated platinum atom.

For isolated Pt_n clusters, an analogous definition for binding energy is used, according to eq 2:

$$E_b = \frac{1}{n}\left(E_{Pt_n} - nE_{Pt_1}\right) \quad (2)$$

where E_{Pt_n} is the energy of the isolated Pt_n cluster.

According to these definitions, the binding energy of the supported system takes into account both the binding energy of isolated Pt_n and its adsorption energy, as already explained in ref 26. Following our definitions, the more negative the binding energy is, the more stable the cluster on the surface.

The adsorption structure of platinum clusters containing 1−5 atoms was studied starting from the most stable positions investigated in the work of Corral Valero et al.[36] for Pd clusters. Similar positions were found stable with Pt, even if new ones were also identified (particularly after migration of OH and Cl). For Pt_{13}, we also used the previous models proposed by C. H. Hu et al.[26,64] In particular, the starting geometries are a biplanar structure on the (100) surface and a three-dimensional one on the (110) surfaces.[26,64]

In addition, we investigated in detail the migration of various species from the (110) surface to the platinum clusters: H, OH (independently and concomitantly), Cl (independently and concomitantly with H atoms). Migration phenomena on the dehydrated (100) surface were not considered due to the absence of OH or Cl surface species. For some specific cases, we also used ab initio molecular dynamics to better explore the various configurations (Supporting Information S5). The barriers for the migration of surface species toward the cluster were not evaluated.

Density of States Analysis. For DOS calculations, the wave function is projected onto spherical harmonics in a sphere around each ion of a specified Wigner−Seitz radius (Al, 1.089 Å; O, 1.485 Å; Pt, 1.695 Å; H, 0.495 Å; Cl, 2.040 Å). Aluminum and oxygen Wigner−Seitz radii were optimized on the bare alumina slab, and the platinum Wigner−Seitz radius was optimized on the bare Pt_{13} cluster supported on an alumina model. The hydrogen Wigner−Seitz radius was optimized on the most stable Pt_3/γ-Al_2O_3(110) (hydrated) system (H and OH migration). Finally, the chlorine Wigner−Seitz radius was optimized on the most stable Pt_3/γ-Al_2O_3(110) (slightly chlorinated) system (H and Cl migration).

■ ASSOCIATED CONTENT

Supporting Information

S1: Binding energies of Pt_n clusters on the alumina surfaces. S2: Interatomic distances. S3: Complementary structures; Pt_{13} supported on hydroxylated and chlorinated surfaces. S4: OH group migration on the hydroxylated surface; strong destabilization of the Pt_1 cluster. S5: Molecular dynamic simulations for investigating the interaction of Pt_{13} on the highly chlorinated surface. S6: Energy decomposition. S7: Complementary Bader charge analysis. This material is available free of charge via the Internet at http://pubs.acs.org.

■ AUTHOR INFORMATION

Corresponding Author

*(P.R.) Phone: +33-4-37-70-23-20. Fax: +33-4-37-70-20-66. E-mail: pascal.raybaud@ifpen.fr. (P.S.) Phone: +33-4-72-72-81-55. Fax: +33-4-72-72-88-60. E-mail: philippe.sautet@ens-lyon.fr

Notes

The authors declare no competing financial interest.

■ ACKNOWLEDGMENTS

Christophe Mager-Maury thanks IFPEN, ENS-Lyon, and ANRT for research grants. Part of this work was performed within the SIRE project (ANR-06-CIS6-014-04) funded by the Agence Nationale de la Recherche (ANR). IFPEN and IDRIS/CINES (GENCI projects x2010086134 and x2011086134) HPC centers are acknowledged for computational time.

■ REFERENCES

(1) Meunier, F. *ACSNano* **2008**, *2*, 2441−2444.
(2) Haruta, M. *Catal. Today* **1997**, *36*, 153−166.
(3) Freund, H.-J. *Surf. Sci.* **2002**, *500*, 271−299.
(4) Bansmann, J.; Baker, S. H.; Binns, C.; Blackman, J. A.; Bucher, J. P.; Dorantes-Dávila, J.; Dupuis, V.; Favre, L.; Kechrakos, D.; Kleibert, A.; Meiwes-Broer, K. H.; Pastor, G. M.; Perez, A.; Toulemonde, O.; Trohidou, K. N.; Tuaillon, J.; Xie, Y. *Surf. Sci. Rep.* **2005**, *56*, 189−275.
(5) Barnes, W. L.; Dereux, A.; Ebbesen, T. W. *Nature* **2003**, *424*, 824−830.
(6) Somorjai, G. A.; Frei, H.; Park, J. Y. *J. Am. Chem. Soc.* **2009**, *131*, 16589−16605.
(7) Vajda, S.; Pellin, M. J.; Greeley, J. P.; Marshall, C. L.; Curtiss, L. A.; Ballentine, G. E.; Elam, J. M.; Catillon-Mucherie, S.; Redfern, P. C.; Mehmood, F.; Zapol, P. *Nat. Mater.* **2009**, *8*, 213−216.
(8) Sanchez, S. I.; Menard, L. D.; Bram, A.; Kang, J. H.; Small, M. W.; Nuzzo, R. G.; Frenkel, A. I. *J. Am. Chem. Soc.* **2009**, *131*, 7040−7054.
(9) Feng, Z.; Kazimirov, A.; Bedzyk, M. J. *ACSNano* **2011**, *5*, 9755−9760.
(10) Jansat, S.; Picurelli, D.; Pelzer, K.; Philippot, K.; Gomez, M.; Muller, G.; Lecantec, P.; Chaudret, B. *New J. Chem.* **2006**, *30*, 115−122.
(11) Farrauto, R. J.; Heck, R. M. *Catal. Today* **1999**, *51*, 351−360.

(12) Sinfelt, J. H. Catalytic Reforming. In *Handbook of Heterogeneous Catalysis*; Ertl, G., Knözinger, E., Weitkamp, J., Eds.; Wiley: Weinheim, 1997; pp 1939−1955.
(13) Chen, A.; Holt-Hindle, P. *Chem. Rev.* **2010**, *110*, 3767−3804.
(14) Huber, G. W.; Cortright, R. D.; Dumesic, J. A. *Angew. Chem., Int. Ed.* **2004**, *43*, 1549−1551.
(15) Euzen, P.; Raybaud, P.; Krokidis, X.; Toulhoat, H.; Loarer, J. L.; Jolivet, J.-P.; Froidefond, C. Alumina. In *Handbook of Porous Solids*; Schüth, F., Sing, K. S. W., Weitkamp, J., Eds.; Wiley-VCH: Weinheim, 2002.
(16) Berdala, J.; Freund, E. *J. Phys. (Paris)* **1986**, *47*, 269−272.
(17) Lynch, J. *Oil Gas Sci. Technol. − Rev. IFP* **2002**, *57*, 281−305.
(18) Marceau, E.; Lauron-Pernot, H.; Che, M. *J. Catal.* **2001**, *197*, 394−405.
(19) Gracia, F. J.; Miller, J. T.; Kropf, A. J.; Wolf, E. E. *J. Catal.* **2002**, *209*, 341−354.
(20) Zhou, Y.; Wood, M. C.; Winograd, N. *J. Catal.* **1994**, *146*, 82−86.
(21) Jahel, A.; Avenier, P.; Lacombe, S.; Olivier-Fourcade, J.; Jumas, J. C. *J. Catal.* **2010**, *272*, 275−286.
(22) Nellist, P. D.; Pennycook, S. J. *Science* **1996**, *274*, 413−415.
(23) Ji, Y.; van der Eerden, A. M. J.; Koot, V.; Kooyman, P. J.; Meeldijk, J. D.; Weckhuysen, B. M.; Koningsberger, D. C. *J. Catal.* **2005**, *234*, 376−384.
(24) Vaarkamp, M.; Miller, J. T.; Modica, F. S.; Koningsberger, D. C. *J. Catal.* **1996**, *163*, 294−305.
(25) Oudenhuijzen, M. K.; van Bokhoven, J. A.; Miller, J. T.; Ramaker, D. E.; Koningsberger, D. C. *J. Am. Chem. Soc.* **2005**, *127*, 1530−1540.
(26) Hu, C. H.; Chizallet, C.; Mager-Maury, C.; Corral Valero, M.; Sautet, P.; Toulhoat, H.; Raybaud, P. *J. Catal.* **2010**, *274*, 99−110.
(27) Deskins, N. A.; Mei, D.; Dupuis, M. *Surf. Sci.* **2009**, *603*, 2793−2807.
(28) Briquet, L. G. V.; Catlow, C. R. A.; French, S. A. *J. Phys. Chem. C* **2008**, *112*, 18948−18954.
(29) Briquet, L. G. V.; Catlow, C. R. A.; French, S. A. *J. Phys. Chem. C* **2009**, *113*, 16747−16756.
(30) Ishimoto, R.; Jung, C.; Tsuboi, H.; Koyama, M.; Endou, A.; Kubo, M.; Del Carpio, C. A.; Miyamoto, A. *Appl. Catal., A* **2006**, *305*, 64−69.
(31) Xiao, L.; Schneider, W. F. *Surf. Sci.* **2008**, *602*, 3445.
(32) Hinnemann, B.; Carter, E. A. *J. Phys. Chem. C* **2007**, *111*, 7105−7126.
(33) Nasluzov, V. A.; Rivanenkov, V. V.; Shor, A. M.; Neyman, K. M.; Rösch, N. *Chem. Phys. Lett.* **2003**, *374*, 487−495.
(34) Kwak, J. H.; Hu, J.; Mei, D.; Yi, C. W.; Kim, D. H.; Peden, C. H. F.; Allard, L. F.; Szanyi, J. *Science* **2009**, *325*, 1670−1673.
(35) Corral Valero, M.; Raybaud, P.; Sautet, P. *J. Phys. Chem. B* **2006**, *110*, 1759−1767.
(36) Corral Valero, M.; Raybaud, P.; Sautet, P. *Phys. Rev. B* **2007**, *75*, 045427 ; 1−12.
(37) Digne, M.; Sautet, P.; Raybaud, P.; Euzen, P.; Toulhoat, H. *J. Catal.* **2002**, *211*, 1−5.
(38) Digne, M.; Sautet, P.; Raybaud, P.; Euzen, P.; Toulhoat, H. *J. Catal.* **2004**, *226*, 54−68.
(39) Digne, M.; Raybaud, P.; Sautet, P.; Guillaume, D.; Toulhoat, H. *J. Am. Chem. Soc.* **2008**, *130*, 11030−11039.
(40) Mei, D.; Kwak, J. H.; Hu, J.; Cho, S. J.; Szanyi, J.; Allard, L. F.; Peden, C. H. F. *J. Phys. Chem. Lett.* **2010**, *1*, 2688−2691.
(41) Mager-Maury, C.; Bonnard, G.; Chizallet, C.; Sautet, P.; Raybaud, P. *ChemCatChem* **2011**, *3*, 200−207.
(42) Valerio, G.; Toulhoat, H. *J. Phys. Chem. A* **1997**, *101*, 1969−1974.
(43) Xu, X.; Kua, J.; Periana, R. A.; Goddard, W. A., III. *Organometallics* **2003**, *22*, 2057−2068.
(44) Frenkel, A. I.; Hills, C. W.; Nuzzo, R. G. *J. Phys. Chem. B* **2001**, *105*, 12689−12703.
(45) Kang, J. H.; Menard, L. D.; Nuzzo, R. G.; Frenkel, A. I. *J. Am. Chem. Soc.* **2006**, *128*, 12068−12069.
(46) Yudanov, I. V.; Metzner, M.; Genest, A.; Rösch, N. *J. Phys. Chem. C* **2008**, *112*, 20269−20275.
(47) Stakheev, A. Y.; Zhang, Y.; Ivanov, A. V.; Baeva, G. N.; Ramaker, D. E.; Koningsberger, D. C. *J. Phys. Chem. C* **2007**, *111*, 3938−3948.
(48) Bus, E.; Miller, J. T.; Kropf, A. J.; Prins, R.; van Bokhoven, J. A. *Phys. Chem. Chem. Phys.* **2006**, *8*, 3248−3258.
(49) Sohlberg, K.; Rashkeev, S.; Borisevich, A. Y.; Pennycook, S. J.; Pantelides, S. T. *ChemPhysChem* **2004**, *5*, 1893−1897.
(50) Alexeev, O. S.; Graham, G. W.; Shelef, M.; Adams, R. D.; Gates, B. C. *J. Phys. Chem. B* **2002**, *106*, 4697−4704.
(51) Perdew, J.; Wang, Y. *Phys. Rev. B* **1992**, *45*, 13244−13249.
(52) Kresse, G.; Hafner, J. *Phys. Rev. B* **1994**, *49*, 14251−14269.
(53) Kresse, G.; Furthmüller, J. *Comput. Mater. Sci.* **1996**, *6*, 15−50.
(54) Kresse, G.; Joubert, D. *Phys. Rev. B* **1999**, *59*, 1758−1775.
(55) Vosko, S. H.; Wilk, L.; Nusair, M. *Can. J. Phys.* **1980**, *58*, 1200−1211.
(56) Henkelman, G.; Arnaldsson, A.; Jonsson, H. *Comput. Mater. Sci.* **2006**, *36*, 354−360.
(57) Krokidis, X.; Raybaud, P.; Gobichon, A. E.; Rebours, B.; Euzen, P.; Toulhoat, H. *J. Phys. Chem. B* **2001**, *105*, 5121−5130.
(58) Paglia, G.; Rohl, A. L.; Buckley, C. E.; Gale, J. D. *Phys. Rev. B* **2005**, *71*, 224115 ; 1−16.
(59) Wolverton, C.; Hass, K. C. *Phys. Rev. B* **2001**, *63*, 024102 ; 1−16.
(60) Joubert, J.; Fleurat-Lessard, P.; Delbecq, F.; Sautet, P. *J. Phys. Chem. B* **2006**, *110*, 7392−7395.
(61) Joubert, J.; Salameh, A.; Krakoviack, V.; Delbecq, F.; Sautet, P.; Copéret, C.; Basset, J. M. *J. Phys. Chem. B* **2006**, *110*, 23944−23950.
(62) Wischert, R.; Copéret, C.; Delbecq, F.; Sautet, P. *Angew. Chem., Int. Ed.* **2011**, *50*, 3202−3205.
(63) Wischert, R.; Copéret, C.; Delbecq, F.; Sautet, P. *Chem. Commun.* **2011**, *47*, 4890−4892.
(64) Hu, C. H.; Chizallet, C.; Toulhoat, H.; Raybaud, P. *Phys. Rev. B* **2009**, *79*, 195416 ; 1−11.